Seismic Response and Fragility Estimates of Highway Bridges Considering Various Modeling Uncertainty Parameters

Huihui Li[1(✉)], Lifeng Li[2], and Liang Xu[3]

[1] Department of Civil Engineering, The City College of New York, New York, NY, USA
`hli004@citymail.cuny.edu`
[2] College of Civil Engineering, Hunan University, Changsha, China
[3] College of Civil Engineering, Chongqing University, Chongqing, China

Abstract. This paper proposes an alternative seismic assessment framework considering various modeling uncertainty parameters, and investigates their effects on the seismic response and seismic fragility estimates of a case-study bridge. Firstly, sensitivity analyses with the tornado diagram technique are performed to determine the sensitivity of some typical bridge engineering demand parameters (EDPs) to twenty-two modeling related uncertain parameters, and the results indicate that the variability in ten identified critical parameters has significant effects on the bridge EDPs. Subsequently, based on a series of nonlinear time history analyses (NLTHAs) on the sample models generated by using Latin hypercube sampling (LHS) method, comparative studies for the seismic responses of some typical bridge members and the seismic fragility estimates both at bridge component and system levels incorporating different levels of uncertainty are performed, respectively. It is concluded that (1) the uncertainty of the modeling related parameters may lead to the difference in the trajectory of seismic response for a given bridge member, whereas the variation of the peak value of such seismic response may due to the joint actions of the uncertainty of ground motions and modeling parameters; (2) the inclusion of only ground motion uncertainty is inadequate and inappropriate, and the proper way is incorporating the uncertainty in those identified significant modeling parameters and ground motions into the seismic response and seismic fragility assessment of highway bridges.

Keywords: Bridges · Seismic fragility analysis · Modeling uncertainty parameters · Sensitivity analysis

1 Introduction

Various sources of uncertainty, such as structural geometric, material, and boundary conditions related parameters may exist due to the structure-to-structure (STS) variation in the seismic fragility assessment of highway bridges (Padgett and DesRoches 2007; Mangalathu and Jeon 2018). Based on the work done by Kiureghian and Ditlevsen (2009), all sources of uncertainty can be categorized into either aleatory uncertainty

or epistemic uncertainty. The former mainly stems from the intrinsic randomness of ground motions, material, static or dynamic forces, and geometric parameters, whereas the latter may derive from the incomplete of statistic data, lack of human knowledge, and several modeling assumptions. One may either ignore the critical uncertain parameters which could lead to the unreliable seismic fragility assessment; or conversely may devote efforts unnecessarily to the computationally expensive simulations which have minimal effects on the seismic response and seismic vulnerability estimates of highway bridges (Padgett and DesRoches 2007). Thus, there is a need for a schematic sensitivity analysis to investigate the effects of the input uncertain parameters and identify the critical parameters on the seismic response and seismic fragility estimates of highway bridges.

Recently, significant research efforts have focused on the investigations of the sensitivity of seismic response and seismic fragility of highway bridges to parameter uncertainty. For example, Padgett and DesRoches (2007) evaluated the sensitivity of seismic responses for some critical bridge components to the uncertainty in the modeling related uncertain parameters, structural geometries, and ground motions by an analysis of variance (ANOVA) technique. Afterward, the sensitivity study was further extended by Padgett et al. (2010) to evaluate the relative importance of 13 random variables on the seismic reliability of critical structural components for steel bridges. Likewise, by taking the steel-concrete composite (SCC) bridges with a dual load path as case-study bridges, Tubaldi et al. (2012) investigated the sensitivity of seismic response and seismic fragility assessment of SCC bridges to the uncertainty in ground motions and 23 modeling related uncertain parameters. They suggested that it is significant to consider the influence of the variability in modeling related uncertain parameters on the safety of SCC bridges. Pang et al. (2014) studied the influence of different sources of uncertainty on the seismic fragility estimates of a cable-stayed bridge, and they found that the seismic vulnerability of the cable-stayed bridge considering the uncertainty in ground motions, structural geometry, and material parameters is more severe than that considering only the uncertainty in ground motions. Similarly, based on a multiparameter fragility model using the Lasso regression technique, Mangalathu and Jeon (2018) found that ignoring the uncertainty in the critical parameters identified from the sensitivity analysis may lead to inaccurate estimates of seismic demand models and seismic fragilities. Therefore, the above-mentioned studies highlight the importance of sensitivity study of the seismic response and fragility estimates of highway bridges to the uncertainty in modeling related uncertain parameters.

The objective of the present study is to (i) identify the critical modeling parameters that impose significant effects on the seismic demand models of the case-study bridge through the sensitivity analysis; (ii) investigate the influence of different levels of uncertainty on the seismic response and seismic fragility estimates of highway bridges; and (iii) suggest an appropriate framework to treat the uncertainty of modeling related uncertain parameters in the seismic response and vulnerability estimates of the highway bridges. Therefore, the current study is organized into several sections. Following this introduction, Sect. 2 focuses on the introduction of the proposed seismic fragility assessment framework considering various modeling related uncertain parameters. Then, Sect. 3 presents the basic information regarding the numerical modeling of

the case-study bridge and summarizes the probabilistic models of 22 modeling related uncertain parameters from three aspects. Subsequently, Sect. 4 performs the sensitivity study of some typical bridge EDPs of the case-study bridge to these 22 modeling parameters and obtains 10 critical parameters through sensitivity analysis with the tornado diagram technique. Next, Sect. 5 investigates the effects of different levels of uncertainty impose on the seismic responses and seismic fragilities both at bridge component and system levels of the case-study bridge. Finally, this study ends with a summary of conclusions in Sect. 6.

2 Seismic Fragility Analysis Considering Various Modeling Uncertainty Parameters

Seismic fragility can be generally defined as the conditional probability of the structural seismic demand, D, exceeding the seismic capacity, C, under different intensity measure (IM) levels. The seismic fragility function can be represented by the following lognormal cumulative distribution function (Li et al. 2020).

$$P(D > C|IM) = \Phi\left\{\frac{\ln[S_D/S_{ci}]}{\sqrt{\beta_{D|IM}^2 + \beta_{ci}^2}}\right\} = \Phi\left[\frac{a + b\ln(IM) - \ln(S_{ci})}{\sqrt{\beta_{D|IM}^2 + \beta_{ci}^2}}\right] \tag{1}$$

where S_D is the median structural seismic demand, S_{ci} is the median structural seismic capacity at i^{th} (i equals 1, 2, 3 and 4) limit state (LS), $\beta_{D|IM}$ is the logarithmic standard deviation of seismic demand, and β_{ci} is the logarithmic standard deviation of seismic capacity at i^{th} limit state, respectively. $\Phi\{\cdot\}$ is the standard normal cumulative distribution function, a and b are the regression coefficients that can be obtained from the linear regression analysis. To simplify the seismic fragility function, Eq. (1) can be further expressed as

$$P_f(LS_i|IM) = \Phi\left[\frac{\ln(IM) - \ln(\lambda)}{\xi}\right] \tag{2}$$

where λ represents the median IM and ξ is the logarithmic standard deviation of the seismic fragility function. Generally, λ and ξ can be used as the seismic fragility parameters to evaluate the seismic fragility of highway bridges, which can be represented as

$$\lambda = e^{[ln(S_{ci})-a]/b}$$
$$\xi = \sqrt{\beta_{D|IM}^2 + \beta_{ci}^2}\Big/ b \tag{3}$$

To incorporate various modeling related uncertain parameters within the seismic fragility assessment framework of highway bridges, $\beta_{D|IM}$ can be expressed as

$$\beta_{D|IM} = \sqrt{\beta_{RTR}^2 + \beta_{Model}^2} \tag{4}$$

where $\beta_{D|IM}$ can be determined by the probabilistic seismic demand analysis (PSDA); β_{RTR} and β_{Model} represent the deviations due to the uncertainty in ground motions

and modeling related uncertain parameters, respectively. Thus, the logarithmic standard deviation of the seismic fragility function can be computed as

$$\xi = \sqrt{\beta_{RTR}^2 + \beta_{Model}^2 + \beta_{ci}^2} \Big/ b \tag{5}$$
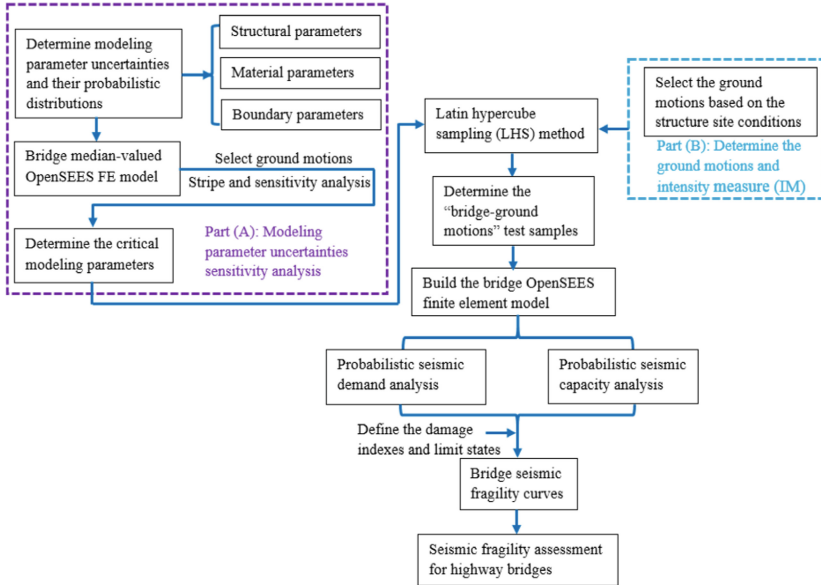
Fig. 1. Seismic fragility assessment framework considering various modeling uncertain parameters.

According to the theory of parameter sensitivity analysis with the tornado diagram technique and seismic fragility modeling, Fig. 1 illustrates the proposed seismic fragility assessment framework considering different modeling uncertainty parameters. As shown in Fig. 1, in part (A), three aspects of modeling related uncertain parameters, such as structural geometric, material, and boundary conditions related parameters, are first determined and then utilized to yield the strip analysis through the median-valued OpenSEES model. Based on the strip analysis, some specific tornado diagrams based sensitivity analyses of some typical EDPs to the modeling uncertainty parameters are performed, and the critical modeling parameters can be determined. Subsequently, in part (B), based on the site condition of the case-study bridge, a series of ground motions and the appropriate IM can be determined. Then, to incorporate the record-to-record (RTR) variability in ground motions, the sample bridge structures are randomly paired with the selected seismic records that used for the seismic fragility analysis by using the Latin hypercube sampling (LHS) method, and a series of "bridge-ground motions" samples are generated. Following this, based on the relevant probabilistic seismic demand and capacity analysis from the finite element (FE) model of the case-study bridge built in the OpenSEES, the seismic fragility curves are developed and utilized for deriving the practical estimates of seismic vulnerability of highway bridges.

3 Bridge Characteristics and the Modeling Related Uncertain Parameters

3.1 Case-Study Bridge and FE Modeling

The case-study bridge shown in Fig. 2 is a representative multi-span reinforced concrete continuous girder (MSRCCG) bridge, which consists of five spans, 30 m each, and a 16 m wide deck supported by four RC circular piers and two RC abutments. The superstructure consists of a 1.8 m high box girder and a cap beam. The height of each pier is 10 m. According to the guidelines for seismic design of Chinese highway bridges (JTG/TB02-01 2008), each pier is reinforced by longitudinal bars and transverse spiral hoops at a reinforcing ratio of 1.08% and 0.58%, respectively. The bridge utilizes the plate-type elastomeric bearing (PTEB) and the lead rubber bearing (LRB) to transfer the forces from the superstructure to substructure through the piers and abutments. The foundation system of each pier consists of nine RC piles with a diameter of 1.5 m and a length of 30 m, and the soil condition belongs to the medium-hard soil profiles.

A general overview of the simulations of some critical bridge components in the OpenSEES database (Opensees Manual 2009) is provided herein. For instance, the composite action of the deck and cap beam is simulated by using the linear elastic beam-column elements since their damages are not expected in the bridge superstructure during the seismic shaking events (JTG/TB02-01 2008). Bridge piers are modeled using nonlinear beam-column elements with fiber defined cross-sections considering the axial force-moment interaction and material nonlinearities. The stress-strain relationship of the confined and unconfined concrete in RC columns are simulated with Concrete 04 material, whereas the longitudinal steel bars, as well as the transverse spiral hoops, are simulated using the Steel 02 material, both of which are available material models in the OpenSEES database (Opensees Manual 2009). Linear translational and rotational springs are utilized to simulate the pile foundations under the piers to capture the translation and rotation behavior of the foundation system. The stiffness of these springs is determined by the "m" method according to the guidelines for the seismic design of Chinese highway bridges (JTG/TB02-01 2008). Moreover, the PTEB and LRB bearings are simulated by using the elastomeric bearing (plasticity) element, and the behavior of abutments is considered by incorporating the contribution of back-fill soil and piles, which can be modeled by using the hyperbolic material and the hysteretic material in the OpenSEES database (Opensees Manual 2009), respectively. Furthermore, the transverse concrete stoppers are simulated by the hysteretic material and elastic-perfectly plastic gap elements. The pounding effect between the deck and abutments can be simulated using the contact element (i.e., nonlinear translational springs) considering the effects of hysteretic energy loss, which can be simulated by the impact materials in the OpenSEES database (Opensees Manual 2009). Thus, the three-dimensional nonlinear dynamic FE model of the case-study bridge and the force-deformation backbone curves of all critical bridge components are presented in Fig. 2.
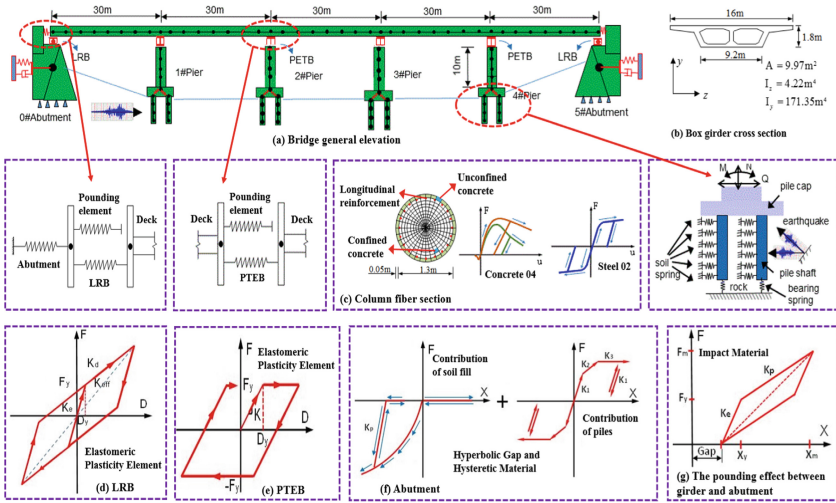
Fig. 2. Nonlinear dynamic FE model of the case-study offshore bridge.

3.2 Modeling Related Uncertain Parameters

The modeling related uncertain parameters considered in this paper mainly include three different aspects, such as (i) structurally related uncertainty (SU) parameters, (ii) material related uncertainty (MU) parameters, and (iii) boundary conditions related uncertainty (BU) parameters. Firstly, SU parameters mainly affect the global dynamic characteristics of the bridge structures. From the perspective of structural dynamics, these uncertainties associated with mass, stiffness, and damping can be attributed to this category, but this paper mainly considers the uncertainty parameters that are related to the geometric dimensions of bridge components and damping ratio. Similarly, MU parameters mainly affect the nonlinear response of bridge columns under the earthquake actions. Due to the superstructure and the cap beam are simulated by the elastic beam-column element, this paper mainly considers the material related uncertain parameters of RC columns. In addition, the case-study bridge considers the complicated nonlinear mechanical properties of bearings (i.e., LRB and PTEB), abutments, and pounding between the girder and the abutments. These nonlinear features are of great importance to the seismic analysis of bridge structures. Therefore, it is necessary to consider the BU parameters. To investigate and quantify the significance of different modeling related uncertain parameters, Table 1 summarizes the associated probability distributions of various modeling related uncertain parameters based on some previous studies.

Table 1. Statistical information on the modeling related uncertainty parameters

Uncertainty parameters	Description	Distribution	Parameter 1	Parameter 2	Reference
λ_w	Concrete weight coefficient	Normal	1.04	10%	Wu et al. (2018), Ma et al. (2019)
D (m)	Pier diameter	Normal	1.4	5%	Padgett et al. (2008), Ma et al. (2019)
c (m)	Concrete cover thickness	Normal	0.05	5%	Padgett et al. (2008), Ma et al. (2019)
ϕ (m)	Longitudinal reinforcement diameter	Normal	28	5%	Padgett et al. (2008), Ma et al. (2019)
ξ	Damping ratio	Normal	0.05	30%	Nielson (2005), Ma et al. (2019)
E_c (MPa)	Young's modulus of concrete	Lognormal	3×10^4	14%	Wu et al. (2018)
$f_{c,cover}$ (MPa)	The peak strength of cover concrete	Lognormal	27.58	20%	Barbato et al. (2010)
$\varepsilon_{c,cover}$	Peak strain of cover concrete	Lognormal	0.002	20%	Barbato et al. (2010)
$\varepsilon_{cu,cover}$	The ultimate strain of cover concrete	Lognormal	0.006	20%	Barbato et al. (2010)
$f_{c,core}$ (MPa)	The peak strength of core concrete	Lognormal	34.47	20%	Barbato et al. (2010)
$\varepsilon_{c,core}$	Peak strain of core concrete	Lognormal	0.005	20%	Barbato et al. (2010)
$\varepsilon_{cu,core}$	The ultimate strain of core concrete	Lognormal	0.02	20%	Barbato et al. (2010)
E_s (MPa)	Young's modulus of steel rebar	Lognormal	2×10^5	5%	Barbato et al. (2010), Pang et al. (2014)

(*continued*)

Table 1. (*continued*)

Uncertainty parameters	Description	Distribution	Parameter 1	Parameter 2	Reference
f_y (MPa)	Yield strength of steel rebar	Lognormal	335	10%	Pang et al. (2014)
γ	Post-yield to initial stiffness ratio	Lognormal	0.02	20%	Barbato et al. (2010)
μ_{PTEB}	The friction coefficient of PTEB	Uniform	0.15	0.25	Wu et al. (2018)
G_{PTEB} (MPa)	Shear modulus of PTEB	Normal	1180	14%	Wu et al. (2018)
K_{P_LRB} (kN/m)	Post-yield stiffness of LRB	Normal	1500	14%	Wu et al. (2018)
P_{ult} (kN)	Abutment ultimate capacity	Uniform	0.5P	1.5P	Nielson (2005), Wu et al. (2018)
$K_{Passive}$ (kN/m)	Abutment passive stiffness	Uniform	0.5K_p	1.5K_p	Nielson (2005), Wu et al. (2018)
K_{Active} (kN/m)	Abutment active stiffness	Uniform	0.5K_A	1.5K_A	Nielson (2005), Wu et al. (2018)
K_{eff} (kN/m)	Pounding effective stiffness	Lognormal	1.94×10^6	14%	Wu et al. (2018)

Note: parameter 1 and parameter 2 represents the mean and coefficient of variation (COV) for the normal and lognormal distributions; lower bound and upper bound for uniform distribution, respectively; P, K_P, and K_A represent the design value of the abutment ultimate capacity, the abutment passive and active stiffness, and $P = 10853$ kN, $K_p = 3.04 \times 10^5$ kN/m, $K_A = 1.86 \times 10^4$ kN/m

4 Sensitivity Analysis of Seismic Response to the Modeling Uncertainty Parameters

4.1 Ground Motions Used for the Sensitivity Analysis

According to the guidelines for the seismic design of Chinese highway bridges (JTG/TB02-01 2008), the case-study bridge requires two probabilistic seismic design

levels of E1 and E2. In which, E1 and E2 seismic design levels need the frequent earthquake evaluation and the rare earthquake evaluation. E1 level of seismic design corresponds to the earthquake with a return period of 475 years, while the E2 level corresponds to the earthquake with a return period of 2500 years. For the ground motions used for the sensitivity analysis in this section, this paper selects 22 pairs of far-field strong earthquake records recommended by the US Federal Emergency Management Agency FEMA-P695 Research Report (FEMA 2009) as the input ground motions. These far-field ground motions were originated from the measured records of 14 major earthquakes that took place between 1971 and 1999. The detailed information for these ground motions can be found in the report (FEMA 2009). According to the given requirements in this report, the original ground motions should be first normalized based on the peak ground velocity (PGV) before using these original records. This is because such a standardized process is significant to reduce the effects of uncertainty in ground motions derived from the magnitude, the epicenter distance, and the site categories. Meanwhile, this normalized procedure can still keep the inherent uncertainty of the selected seismic records. Figure 3 displays the scaling of the selected ground motions under the probabilistic seismic design levels of E1 and E2 in the guidelines for seismic design of Chinese highway bridges (JTG/TB02-01 2008).
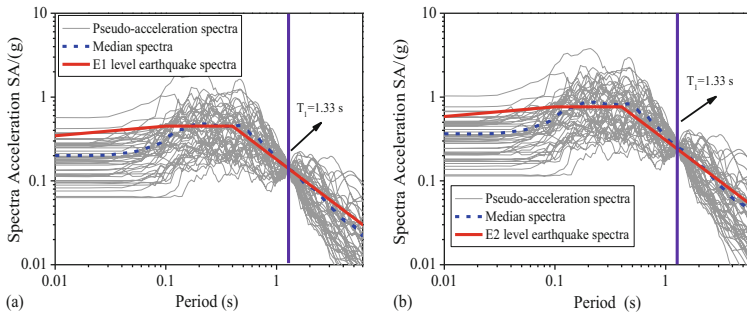
Fig. 3. Response spectra of ground motions for sensitivity analysis: (a) E1 level and (b) E2 level.

As shown in Fig. 3, corresponding to the case-study bridge fundamental period of T_1 = 1.33 s, the spectral acceleration (SA) of the selected 22 pairs of ground motions after scaling is matching well with the standard spectral acceleration. It should be mentioned herein that the recommended seismic records in FEMA report (FEMA 2009) are derived from the strong earthquake database of the Pacific Earthquake Engineering Research Centre Ground Motion Database (PEER Ground Motion Database 2015) and each pair of seismic record contains both FP (Fault Parallel) and FN (Fault Normal) directions. Furthermore, due to the differences in spectral characteristics for each pair of seismic record, the corresponding PGA, PGV, and SA are inconsistent and varied. Thus, each pair of the seismic record should be considered as two independent ground motions, and a total of 44 ground motions are utilized for the following sensitivity analysis.

4.2 Sensitivity Analysis of Seismic Response to Different Modeling Uncertainty Parameters

It is necessary to investigate the effects of various uncertain parameters on some typical EDPs (as presented in Table 2) of the case-study bridge, and based on a series of previous studies (Porter et al 2002; Celik and Ellingwood 2010; Zhong et al. 2018; Wu et al. 2018), sensitivity analyses of seismic responses for different bridge components to the modeling related uncertain parameters are performed herein using the tornado diagram technique.

Table 2. Bridge engineering demand parameters (EDPs)

ID	Seismic demand parameters	Variable	Unit	Note
1	The curvature of the column	Φ_L	m^{-2}	Longitudinal
2	The relative displacement of LRB	δ_{LRB_L}	cm	Longitudinal
3	The relative displacement of PTEB	δ_{PTEB_L}	cm	Longitudinal
4	Abutment deformation	Δ_{Abut_active}	cm	Active
5	Abutment deformation	$\Delta_{Abut\_passive}$	cm	Passive

According to the work done by Celik and Ellingwood (2010), Zhong et al. (2018), and Wu et al. (2018), sensitivity analysis with the tornado diagram technique can be performed as following. Firstly, all of the considered modeling related uncertain parameters listed in Table 1 are set equal to their respective median values, and then 44 nonlinear time history analyses (NLTHAs) are conducted to develop the median-valued model for the critical EDPs listed in Table 2. Then, this procedure is carried out repeatedly for each of the 22 modeling related uncertain parameters, in turn, varying only one at a time and setting each parameter to its lower bound (5th percentile) and upper bound (95th percentile) while holding the remaining parameters at their median values. Furthermore, after a series of NLTHAs are performed, the variation in median values of the seismic responses with each modeling uncertain parameter can be displayed through a tornado diagram (Porter et al 2002; Celik and Ellingwood 2010; Zhong et al 2018). For example, Figs. 4, 5, 6, 7 and 8 illustrate the tornado diagrams for the seismic responses, Φ_L, δ_{LRB_L}, δ_{PTEB_L}, Δ_{Abut_active}, and $\Delta_{Abut\_passive}$, under E1 and E2 designed levels of ground motions. However, it should be noted that the NLTHAs may fail to converge for some ground motions when they are scaled to a higher seismic hazard event (i.e., E2 design level). For such cases, the maximum likelihood function can be used to estimate the parameters of the lognormal probability distribution (Celik and Ellingwood 2010). This paper presents only a brief introduction of the sensitivity analysis using the tornado diagram technique, interested readers can refer to more relevant works (Celik and Ellingwood 2010; Zhong et al. 2018).
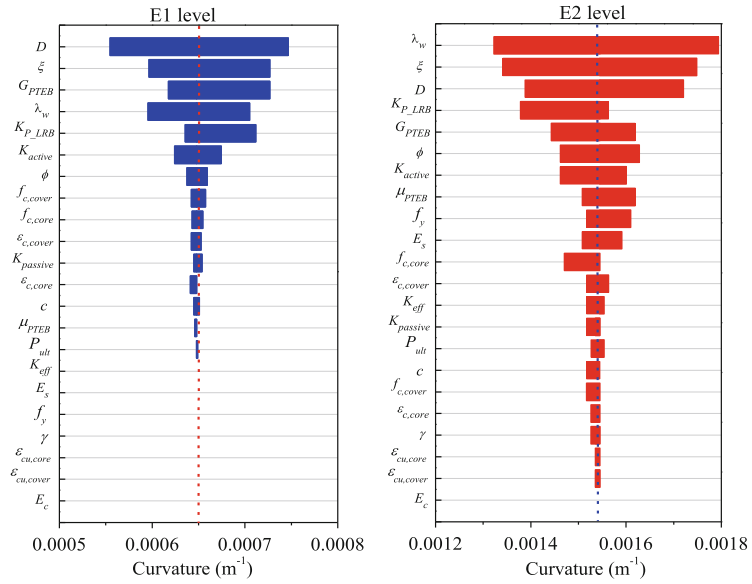
Fig. 4. Tornado diagrams for pier curvature (Φ_L) under different levels of ground motions.
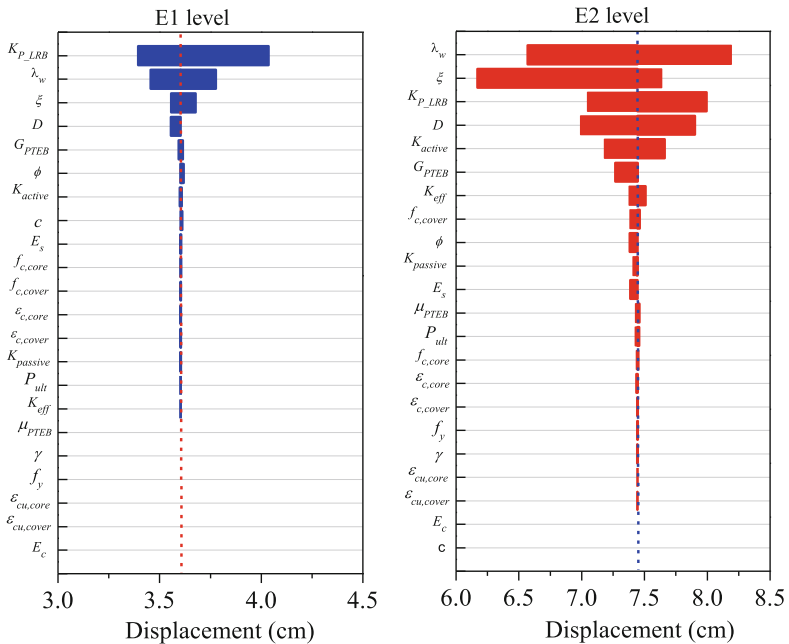
Fig. 5. Tornado diagrams for the displacement of LRB (δ_{LRB_L}) under different levels of ground motions.
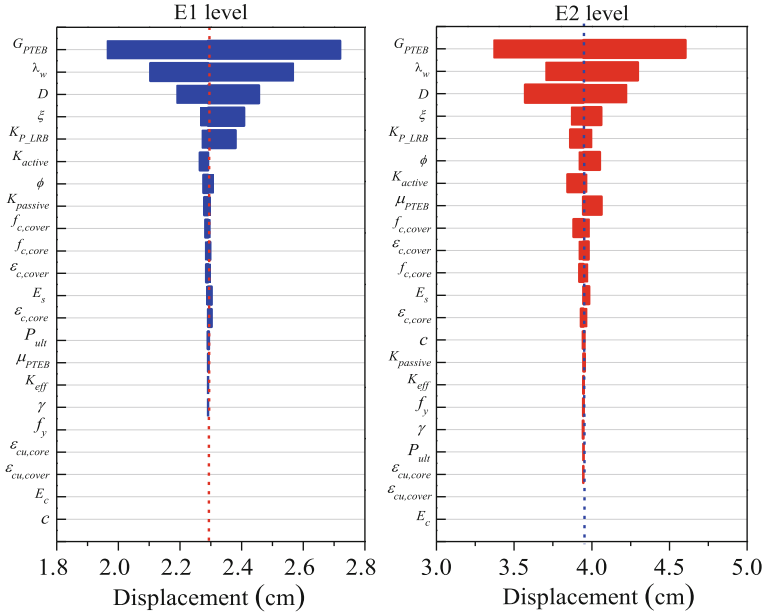
Fig. 6. Tornado diagrams for the displacement of PTEB (δ_{PTEB_L}) under different levels of ground motions.
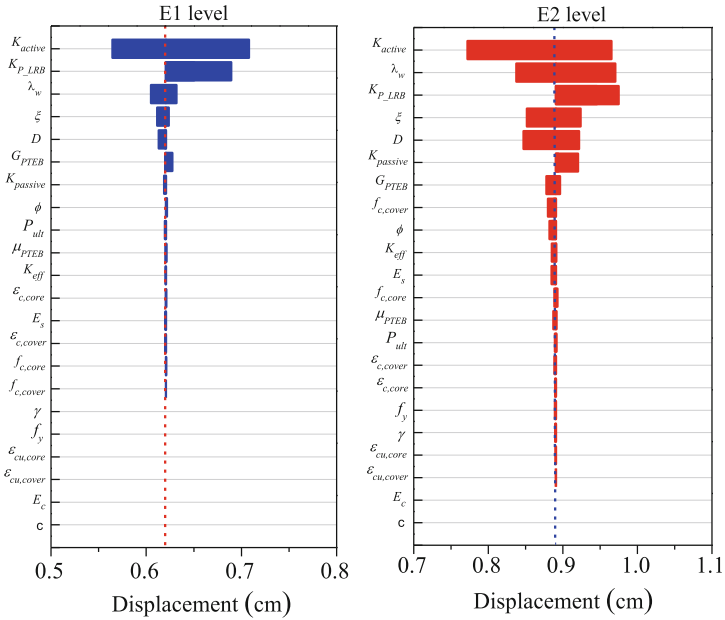
Fig. 7. Tornado diagrams for the displacement of abutment-active (Δ_{Abut_active}) under different levels of ground motions.
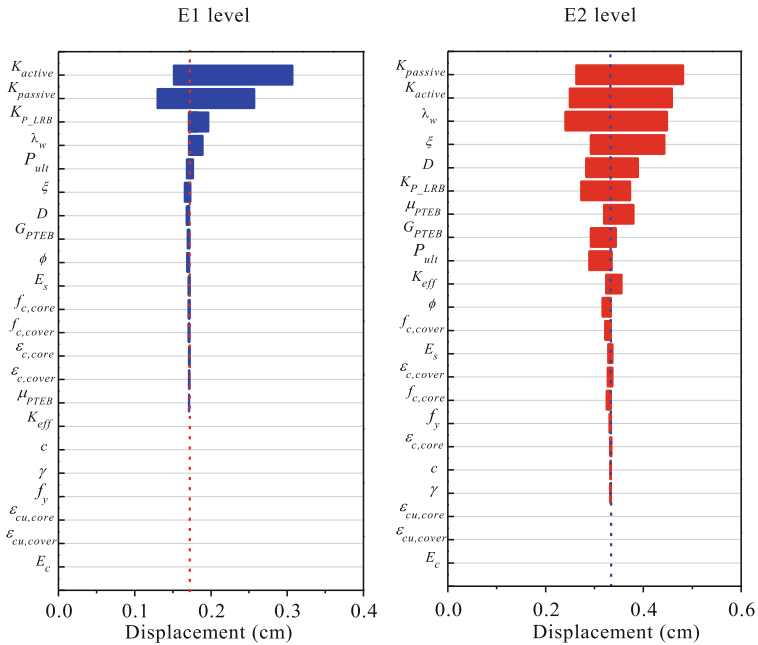
Fig. 8. Tornado diagrams for the displacement of abutment-passive ($\Delta_{Abut\_passive}$) under different levels of ground motions.

Table 3. Critical modeling uncertain parameters obtained from the sensitivity analysis

ID	Uncertain parameters	Description
1	λ_w	Concrete weight coefficient
2	D (m)	Pier diameter
3	φ (mm)	Longitudinal reinforcement diameter
4	ξ	Damping ratio
5	$f_{c,\,cover}$	The peak stress of cover concrete
6	μ_{PTEB}	The friction coefficient of PTEB
7	G_{PTEB} (MPa)	Shear modulus of PTEB
8	K_{P_LRB} (kN/m)	Post-yield stiffness of LRB
9	$K_{passive}$ (kN/m)	Abutment passive stiffness
10	K_{active} (kN/m)	Abutment active stiffness

As seen from Fig. 4 to Fig. 8, for a specific tornado diagram, the length of the histogram in a tornado diagram identifies the influential effect of the modeling related uncertain parameter, and the longer the histogram is the more significant of the modeling uncertain parameter is (Celik and Ellingwood 2010). It can be observed from Fig. 4 to Fig. 8 that the effects of different modeling related uncertain parameters impose on the seismic responses of different bridge components are significantly varied. Thus, it is necessary to consider the influence of various modeling uncertainty parameters. Sensitivity analysis through the tornado diagram technique provides new insight into the identification of the critical modeling parameters. By counting the total number of times each modeling parameter has been ranked in the top ten, we can obtain the corresponding critical parameters as summarized in Table 3, while the rest of the random parameters have much smaller or no discernible effects on the seismic responses of the given bridge components. Therefore, these 10 identified critical parameters are suggested to be regarded as random variables, while the uncertainty in the other 12 remaining parameters can be neglected without resulting in a significant loss of accuracy. Thus, these 12 remaining parameters can be set to their median values (deterministic) in the FE models used for the following seismic fragility analysis of the case-study bridge.

5 Effects of Modeling Uncertainty Parameters on the Seismic Response and Fragility Estimates of the Case-Study Bridge

5.1 Effects of Modeling Related Uncertain Parameters on the Seismic Responses

To qualitatively investigate the influence of various modeling uncertainty parameters on the nonlinear seismic responses of the case-study bridge, Fig. 9 performs a comparative study of seismic hysteretic responses for different bridge components obtained by using the NLTHAs under two different ground motions (i.e., Northridge and Kobe). The acceleration time histories of these two seismic records are displayed in Fig. 10. As shown in Fig. 9, the given nonlinear seismic hysteretic curves with two levels of uncertainty are developed under two different ground motions. In which, uncertainty case 1 and case 2 can be termed as "RTR only" and "RTR+All", respectively. Case 1 ("RTR only") incorporates only the uncertainty in the ground motions and set all of the modeling related uncertain parameters listed in Table 1 equal to their median values, while case 2 ("RTR+All") considers both the uncertainty of ground motions and all of the modeling parameters listed in Table 1. Since all of the modeling related uncertain parameters in case of "RTR only" equal to their respective median values (deterministic), this case herein can be defined as the "Deterministic model", which only considers the uncertainty in ground motions. However, since all of the modeling related uncertain parameters in case of "RTR+All" are treated as random variables, this case is defined as the "Stochastic model", which considers both the uncertainty in ground motions and the modeling related uncertain parameters.

As seen from Fig. 9(a1), (b1), (c1) and (d1), for the "Deterministic model", due to the uncertainty of seismic records, the peak value of nonlinear seismic hysteretic response for each component of the case-study bridge is different, while the trajectory of seismic hysteretic response for each bridge component is almost the same under the action of
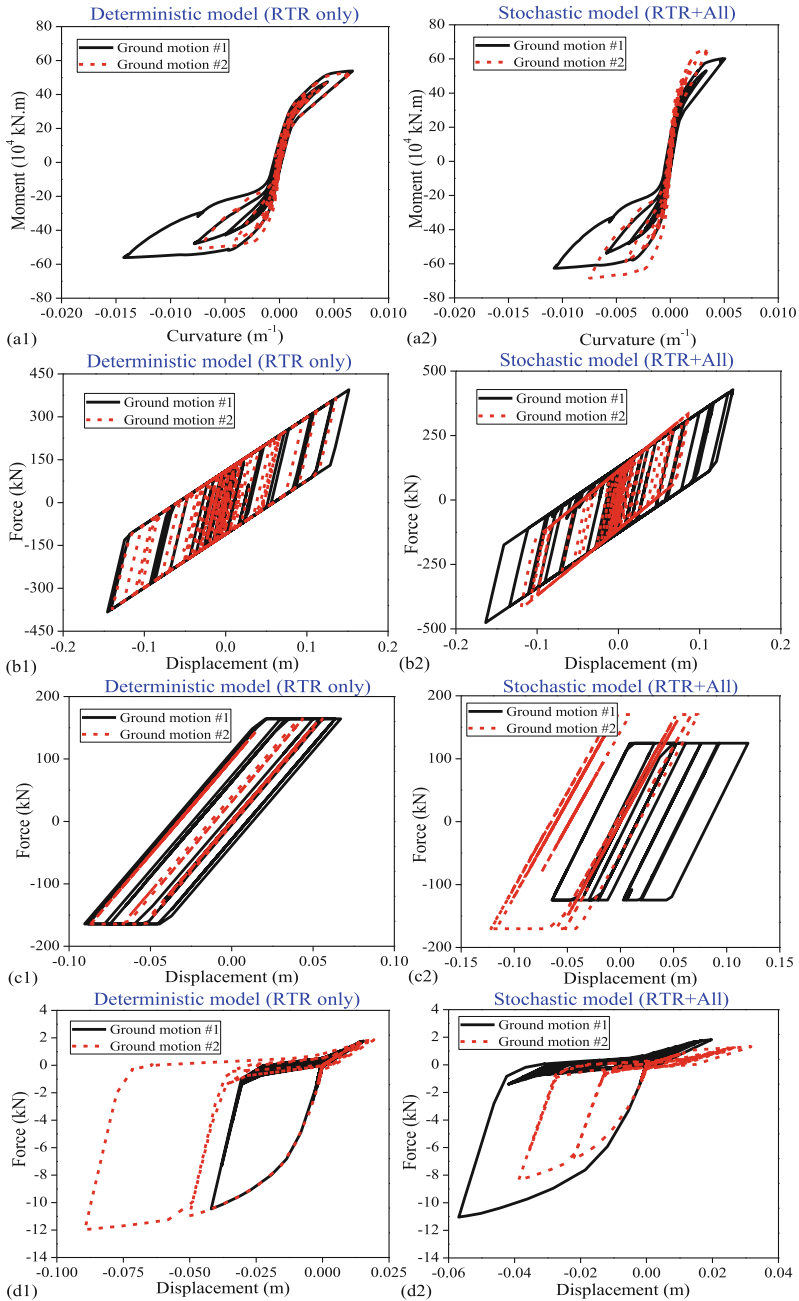
Fig. 9. Seismic responses for different components of the pristine case-study bridge under two different ground motions: (a) pier, (b) LRB, (c) PTEB, and (d) abutment.
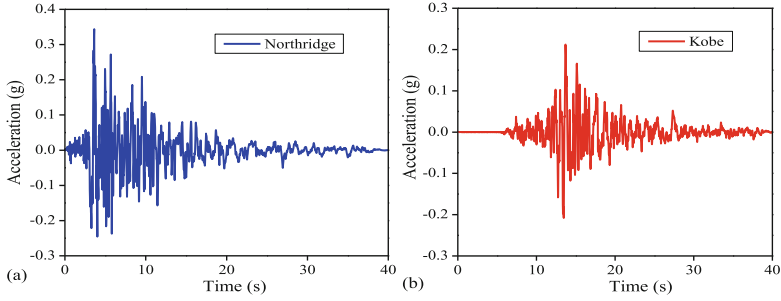
Fig. 10. Acceleration time history curve for (a) ground motion #1: Northridge and (b) ground motion #2: Kobe seismic record.

Northridge and Kobe seismic records. However, from Fig. 9(a2), (b2), (c2) and (d2), as for the "Stochastic model", under the impact caused by the uncertainty both of the ground motions and all of the modeling related uncertain parameters, not only the peak value but also the trajectory of seismic hysteretic response for each bridge member may vary with the input ground motions. These findings indicate that the difference of the trajectory of seismic hysteretic response for a specific bridge component may due to the uncertainty of modeling parameters, whereas the variation of the peak seismic response could be caused by the joint actions of the uncertainty of ground motions and modeling related uncertain parameters.
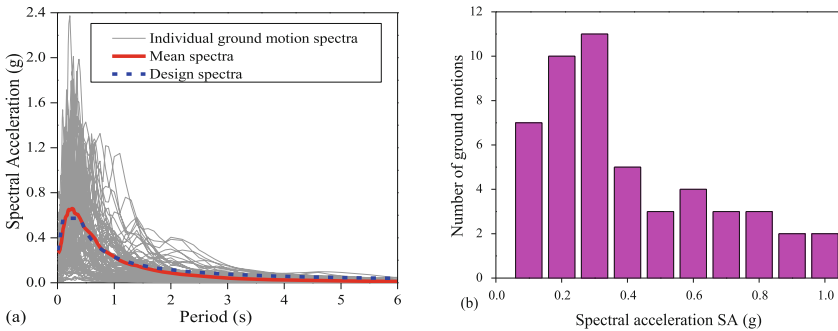
Fig. 11. Response spectra of the selected ground motions used for the seismic fragility analysis of the case-study bridge.

5.2 Ground Motions and Limit States

The selection of ground motions is critical to provide a good prediction of seismic response for highway bridges. According to the site condition of the case-study bridge, this paper selects 50 pairs of seismic records from the PEER Centre Ground Motion Database (PEER Ground Motion Database 2015) as the input ground motions used for the following seismic fragility analysis. Figure 11(a) shows the response spectra of the

selected ground motions. It is observed that the mean value of the acceleration spectra of the selected seismic records is well matching with the design spectra for the case study bridge (JTG/TB02-01 2008). For the regular RC girder bridges that are similar to the case-study bridge, the seismic response is mainly dominated by the first mode of dynamic analysis. As a consequence, the 5% damped first-mode spectral acceleration (SA) is employed as the intensity measure for the seismic fragility analysis in this study (Li et al. 2020). Figure 11(b) shows the distribution of SA values for the selected ground motions. Thus, it can be observed that the selected seismic records cover a relatively broad range of SA values. For the selected seismic records, their moment magnitudes vary from 6.5 to 7.5 and their hypo-central distances range from 15 and 100 km. This shows that the selected ground motions can represent both small and large earthquakes with different epicentral distances.

Table 4. Damage indexes of different bridge components under different limit states.

Components	SL		MO		EX		CO	
	S_c	β_c	S_c	β_c	S_c	β_c	S_c	β_c
μ_ϕ	1.0	0.127	2.21	0.246	5.40	0.472	11.12	0.383
μ_z	1.0	0.246	1.5	0.246	2.0	0.472	2.5	0.472
γ_a	100%	0.246	150%	0.246	200%	0.472	525%	0.472
δ_{active} (mm)	13	0.246	26	0.246	78	0.472	150	0.472
$\delta_{passive}$ (mm)	5.5	0.246	11	0.246	35	0.472	100	0.472

Within the performance-based earthquake engineering (PBEE) framework, the most widely accepted limit state definitions are proposed by HAZUS (1999), which defines four limit states, such as slight (SL), moderate (MO), extensive (EX) and complete (CO) limit states. According to several previous studies (Nielson 2005; Pan et al. 2007), the ductility factor can be utilized as the damage index of concrete components, whereas for other bridge components, such as abutments and bearings can be indicated by the relative displacement or shear strain. This study considers the damage of RC pier, LRB, PTEB, and abutment. Hence, based on the studies of Nielson (2005), the defined damage indexes under different limit states for different bridge components are summarized in Table 4, where μ_Φ is the curvature ductility at the base section of the columns, μ_z is the displacement ductility of PTEB, γ_a is the allowable shear strain of LRB, δ_{active} and $\delta_{passive}$ is the active and passive displacement of the abutment, respectively.

5.3 Effects of Modeling Related Uncertain Parameters on the Seismic Fragilities

According to the proposed seismic fragility analysis framework in Sect. 2, the seismic fragility curves of different bridge components can be developed as shown in Fig. 12. As seen from Fig. 12, LRB is the most fragile component at the former three limit states, and the failure probability of LRB is much higher than that of PTEB. This may because the lateral stiffness of piers is less than that of the abutment, so the relative displacement

of LRB under the earthquake excitation is much less than that of PTEB. However, in Fig. 12(d), the failure probability of LRB at CO damage state is less than that of PTEB, which may result from the damage of LRB at this condition is not be determined by the damage of the bearing itself but the girder falling during the seismic shaking events. In addition, it should be noted that the fragility curves of the abutment passive direction at the latter two damage states are relatively flat, which may be a consequence of the complicated pounding effects imposed by the deck and abutments.

Generally, both the seismic fragility curves and fragility parameters (λ and ξ in Eq. (3)) can be utilized to assess the seismic vulnerabilities of highway bridges. Thus, to investigate the effects of incorporating different levels of uncertainty in modeling related uncertain parameters on the seismic fragility estimates of the case-study bridge, three cases of uncertainty treatment are taken into consideration. Apart from two uncertainty level cases ("RTR only" and "RTR+All") that have mentioned in Sect. 5.1, a third case termed as "RTR+Critical" is also considered herein. To be specific, "RTR+Critical" incorporates the uncertainty in ground motions along with the uncertainty of these 10 critical parameters (Table 3) identified from the sensitivity analysis, while the other 12 remaining parameters in Table 1 equal to their respective median values. To examine the influence of including different levels of uncertainty in modeling related uncertainty parameters on component seismic fragilities, and due to the failure probabilities for bridge components under EX and CO damage state are relatively small (as seen from Fig. 12), Fig. 13 only compares the median SA (corresponding to 50% failure probability) under SL and MO damage states.
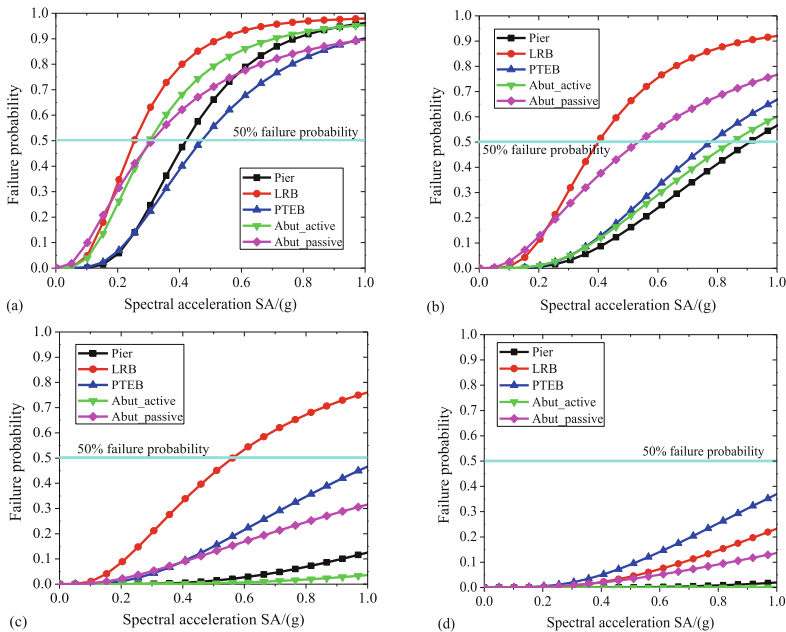
Fig. 12. Bridge component seismic fragility curves: (a) SL, (b) MO, (c) EX, and (d) CO damage state.
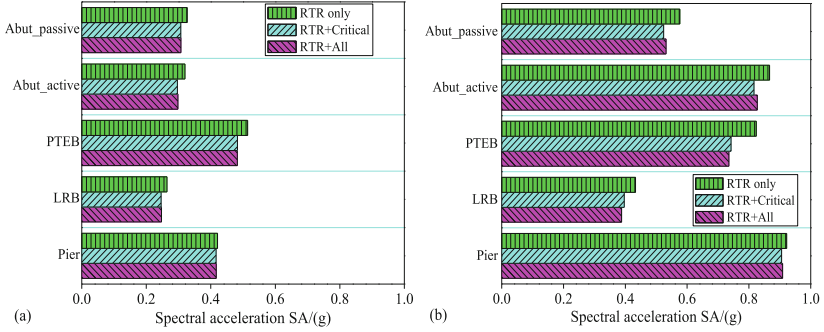
Fig. 13. Median SA of different bridge members with different levels of uncertainty: (a) SL (b) MO damage state.

As observed from Fig. 13, compared to the median SA considering only the uncertainty in the ground motions (case "RTR only"), there is a relatively significant difference from those considering additional uncertainty of critical or all modeling related uncertain parameters, and the difference tends to increase with the severity of limit states. However, the difference between the set of fragility parameters (median SA) incorporating the uncertainty in ground motions as well as the critical parameters (case "RTR+Critical") and those with the additional uncertainty in the remaining 12 parameters (case "RTR+All") are very little. This indicates that the bridge component seismic fragilities are sensitive to these 10 critical parameters identified in the preceding sensitive analysis but much less sensitive to the remaining 12 modeling parameters. In addition, the influence of uncertainty levels on the seismic fragility of different bridge components is varied. For example, the impact due to different cases of uncertainty treatment on the seismic fragility of the pier is relatively minor to those on other bridge components, such as LRB, PTEB, and abutment.

Similarly, to investigate the effect of different cases of uncertainty treatment impose on the logarithmic standard deviation ξ in the seismic fragility function, Table 5 shows the uncertainty in the corresponding logarithmic standard deviations of different bridge components. As seen from Table 5, both the deviations result from the uncertainty in ground motions (β_{RTR}) and modeling related parameters (β_{Model}) are varied with the bridge EDPs. From an overall perspective, β_{Model} are less than β_{RTR} for all bridge components, and the range for β_{Model} and β_{RTR} of the case-study bridge is 0.251 to 0.456 and 0.310 to 0.671, respectively. Moreover, the fragility parameters (ξ) for all bridge components tend to increase with the severity of limit states, and ξ for both the active and passive direction of abutment are relatively larger than that for other bridge members. This may result from the complicated and nonlinear pounding or impact that occurs between the deck and abutments. However, to investigate the effects imposed by the uncertainty in ground motions and modeling related uncertain parameters on the deviations of different bridge components, Fig. 14 compares the contributions of β_{RTR}, $\beta_{Model\_All\ parameters}$, and $\beta_{Model\_Critical\ parameters}$ on different bridge EDPs. From Eq. (4) in Sect. 2, we can calculate β_{Model} by the following equation as

$$\beta_{Model} = \sqrt{\beta_{D|IM}^2 - \beta_{RTR}^2} \qquad (6)$$

Table 5. Uncertainty in logarithmic standard deviations for different bridge components.

Component	β_{RTR}	β_{Model}	$\beta_{D|IM}$	β_{ci}	ξ
Pier	0.310	0.251	0.399	0.127	0.402
				0.274	0.463
				0.321	0.488
				0.383	0.529
LRB	0.247	0.198	0.317	0.246*	0.473
				0.472**	0.675
PTEB	0.284	0.224	0.362	0.246*	0.522
				0.472**	0.714
Abut_active	0.389	0.339	0.516	0.246*	0.725
				0.472**	0.856
Abut_passive	0.671	0.456	0.811	0.246*	0.753
				0.472**	0.828

Note: where $\beta_{D|IM} = \sqrt{\beta_{RTR}^2 + \beta_{Model}^2}$, $\xi = \sqrt{\beta_{D|IM}^2 + \beta_{ci}^2}\big/b$; "*" represents the deviations for SL and MO damage states, and "**" denotes the deviations EX and CO damage states

where $\beta_{D|IM}$ can be obtained by PSDA and when $\beta_{D|IM}$ equals to β_{RTR}, β_{Model} equals 0. This corresponds to the case of uncertainty treatment ("RTR only") when all the modeling related uncertain parameters are set to their median values. $\beta_{Model\_All\ parameters}$ and $\beta_{Model\_Critical\ parameters}$ can be determined through Eq. (6) by considering the uncertainty in all of the modeling parameters or only the critical modeling related parameters. As shown in Fig. 14, for all bridge members, compared to the influence of β_{RTR} on different bridge EDPs, there is a relatively significant difference from those of β_{Model}. However, the differences between $\beta_{Model\_All\ parameters}$ and $\beta_{Model\_Critical\ parameters}$ are very little. This indicates that the deviations are sensitive to these 10 significant modeling parameters but much less sensitive to the remaining 12 parameters.

Likewise, to investigate the effect of modeling uncertainty parameters on the bridge system-level seismic fragility, Fig. 15 compares the seismic fragility curves and the median SA plots with three different levels of uncertainty. As observed from Fig. 15, similar results about the influence generated by different levels of uncertainty in modeling related uncertain parameters on the system-level seismic fragility can be found similar to that on the bridge component-level seismic vulnerability. Therefore, based on the above analysis, the results suggest that the inclusion of only the uncertainty derived from the ground motions (case "RTR only") may not sufficient to evaluate the seismic fragility of highway bridges, and it is necessary to take into consideration the uncertainty contributions of different modeling related uncertain parameters. The results also indicate that we can reduce the number of NLTHA simulations for PSDA and thereby
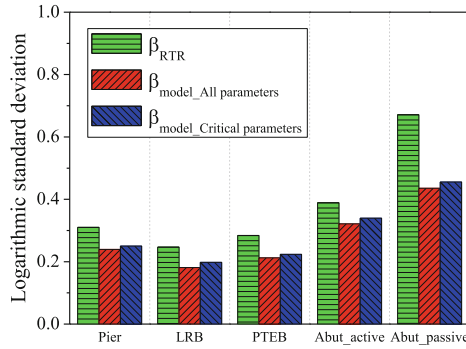
Fig. 14. The logarithmic standard deviation of bridge components with a different source of uncertainty.
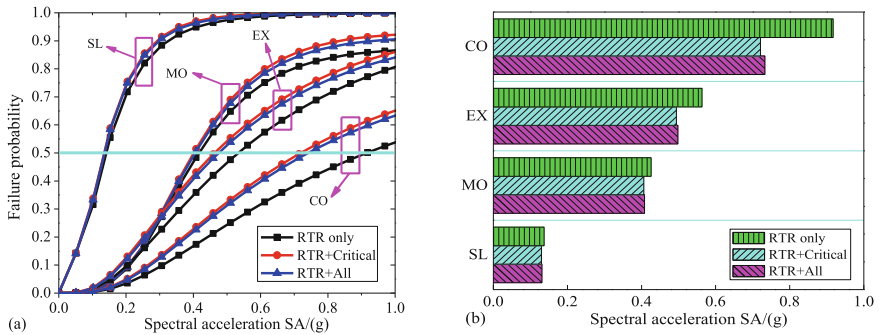
Fig. 15. System seismic fragility curve and fragility parameter with different levels of uncertainty.

save time as well as the computational efforts by considering only the critical modeling related parameters identified through the sensitivity analysis in the future seismic fragility assessment of highway bridges. Such a method in identification of significant modeling parameters by sensitivity analysis with the tornado diagram technique helps bridge owners and engineers to identify the critical variables to pay attention to the design and corresponding seismic performance evaluation of highway bridges.

6   Conclusion

This paper proposes a schematic seismic fragility assessment framework for highway bridges considering various modeling related uncertain parameters. A total of twenty-two random variables are probabilistically characterized to represent the modeling related uncertain parameters from three different aspects. A variety of bridge EDPs are employed as measures to investigate the sensitivity of the seismic responses of the case-study bridge to these modeling uncertainty parameters. Then, ten critical modeling parameters are identified through the sensitivity analysis with the tornado diagram technique, and these critical parameters are suggested to be treated as random variables, while the remaining

12 parameters can be selected as deterministic by set equal to their respective median values. In addition, the findings of the sensitivity analysis are extended to investigate the influence of incorporating different levels of uncertainty on the seismic response and seismic fragility estimates both at bridge component and system levels. Finally, the following conclusions can be summarized as.

(1) The difference of the trajectory of seismic hysteretic response for a specific bridge component may vary due to the uncertainty of modeling related uncertain parameters, whereas the variation of the peak seismic response may vary due to the joint contributions of the ground motion uncertainty and modeling parameters variability.
(2) It is essential to consider the variability of the identified significant modeling parameters from the sensitivity analysis because the uncertainty in these critical parameters has considerable effects on the seismic demand models, seismic response, and seismic fragility estimates of highway bridges.
(3) The differences of the developed bridge component and system-level seismic fragilities between the case of "RTR+Critical" and "RTR+All" are negligible. Thus, sensitivity analysis with the tornado diagram technique is a good candidate method to identify the critical modeling parameters, and it helps reduce the number of nonlinear simulations and minimizing the computational efforts in the seismic response and fragility estimates of highway bridges.

References

Barbato, M., Gu, Q., Conte, J.P.: Probabilistic push-over analysis of structural and soil-structure systems. J. Struct. Eng. **136**(11), 1330–1341 (2010)

Celik, O.C., Ellingwood, B.R.: Seismic fragilities for non-ductile reinforced concrete frames - role of aleatoric and epistemic uncertainties. Struct. Saf. **32**(1), 1–12 (2010)

FEMA: Quantification of building seismic performance factors. Applied Technology Council, Federal Emergency Management Agency: Washington, D.C. (2009)

HAZUS: Earthquake loss estimation methodology, SR2 edition. National Institute of Building Sciences for Federal Emergency Management Agency, Washington D.C. (1999)

Kiureghian, A.D., Ditlevsen, O.: Aleatory or epistemic? Does it matter? Struct. Saf. **31**(2), 105–112 (2009)

Li, H., Li, L., Wu, W., Xu, L.: Seismic fragility assessment framework for highway bridges based on an improved uniform design-response surface model methodology. Bull. Earthq. Eng. **18**(5), 2329–2353 (2020). https://doi.org/10.1007/s10518-019-00783-1

Ma, H.-B., et al.: Probabilistic seismic response and uncertainty analysis of continuous bridges under near-fault ground motions. Front. Struct. Civ. Eng. **13**(6), 1510–1519 (2019). https://doi.org/10.1007/s11709-019-0577-8

Mangalathu, S., Jeon, J.S.: Critical uncertainty parameters influencing the seismic performance of bridges using Lasso regression. Earthq. Eng. Struct. Dyn. **47**(3), 784–801 (2018)

Ministry of Communications of PRC: Guidelines for seismic design of highway bridges (JTG/TB02-01). Beijing: China Communications Press (2008). (in Chinese)

Nielson, B.G.: Analytical fragility curves for highway bridges in moderate seismic zones. Ph.D. thesis, Georgia Institute of Technology, Atlanta, United States (2005)

Opensees Manual: Open system for earthquake engineering simulation user command-language manual. Pacific Earthquake Engineering Research Center, University of California, Berkeley, United States (2009)

Padgett, J.E., DesRoches, R.: Sensitivity of seismic response and fragility to parameter uncertainty. J. Struct. Eng. **133**(12), 1710–1718 (2007)

Padgett, J.E., Ghosh, J., Dueñas-Osorio, L.: Effects of liquefiable soil and bridge modeling parameters on the seismic reliability of critical structural components. Struct. Infrastruct. Eng. **9**(1), 59–77 (2010)

Padgett, J.E., Nielson, B.G., DesRoches, R.: Selection of optimal intensity measures in probabilistic seismic demand models of highway bridge portfolios. Earthq. Eng. Struct. Dyn. **37**(5), 711–725 (2008)

Pan, Y., Agrawal, A.K., Ghosn, M.: Seismic fragility of continuous steel highway bridges in New York State. J. Bridge. Eng. **12**(6), 689–699 (2007)

Pang, Y.T., Wu, X., Shen, G.Y., et al.: Seismic fragility analysis of cable-stayed bridges considering different sources of uncertainties. J. Bridg. Eng. **19**(4), 1–11 (2014)

PEER Ground Motion Database: PEER (Pacific Earthquake Engineering Research Center) (2015). http://ngawest2.Berkeley.edu/site

Porter, K.A., Beck, J.L., Shaikhutdinov, R.V.: Sensitivity of building loss estimates to major uncertain variables. Earthq. Spectra. **18**(4), 719–743 (2002)

Tubaldi, E., Barbato, M., Dall'Asta, A.: Influence of model parameter uncertainty on seismic transverse response and vulnerability of steel-concrete composite bridges with dual load path. J. Struct. Eng. **138**(3), 363–374 (2012)

Wu, W.P., Li, L.F., Tang, S.H., Zhang, X.H.: Sensitivity investigation of modeling uncertainty for seismic demand analysis of bridges. J. Vib. Shock. **37**, 257–270 (2018). (in Chinese)

Zhong, J., Zhi, X.D., Fan, F.: Sensitivity of seismic response and fragility to parameter uncertainty of single-layer reticulated domes. Int. J. Steel. Struct. **18**(5), 1607–1616 (2018)